



# Bio-engineered of Zirconium Dioxide (ZrO<sub>2</sub>) Nanoparticles from *Caulerpa scalpelliformis* algae Extract, Characterization and their Antimicrobial Applications

Parthiban. V<sup>1\*</sup>, Rajani Kumar K<sup>3,4</sup>, Dr. N. Chandra Lekha<sup>2</sup>, Dr. K. Uday kumar<sup>3</sup>

<sup>1\*</sup>Research Scholar, Department of Chemistry, Kamaraj College, Thoothukudi. (Affiliated to M.S University, Tirunelveli)

<sup>3\*</sup>Research Scholar, Department of Physics, National Institute of Technology, Warangal, Telangana, India.

<sup>2</sup>Department of Chemistry, Kamaraj College, Thoothukudi

<sup>3</sup>Department of Physics, National Institute of Technology, Warangal, Telangana, India.

<sup>4</sup>109 nano composite technologies private limited, Guntur, Andhra Pradesh, India.

**Abstract :** Zirconium dioxide nanoparticles (ZrO<sub>2</sub> NPs) were successfully made in this study using a green synthesis approach by combining *Caulerpa scalpelliformis* algae extract with zirconium nitrate salt (ZrO (NO<sub>3</sub>)<sub>2</sub> H<sub>2</sub>O) at 250 °C for two hours. ZrO (NO<sub>3</sub>)<sub>2</sub> H<sub>2</sub>O is changed into Biomolecules found inside the extract, such as ZrO<sub>2</sub> NPs, are crucial. By using X-ray diffraction (XRD), Fourier transform infrared (FTIR), scanning electron microscopy (SEM), Energy dispersive X-Ray (EDX) composition analysis, and an ultraviolet-visible (UV-Vis) spectrophotometer, the generated ZrO<sub>2</sub> NPs were examined. The generated ZrO<sub>2</sub> NPs are polycrystalline with mixed-phase systems (tetragonal and monoclinic), with a crystallite size of around 5 nm, according to X-ray diffraction data of the nanoparticles. The FTIR spectra, which showed monoclinic and tetragonal phase, supported the XRD findings. The synthetic approach was shown to be very cost-effective, efficient, and environmentally benign. ZrO<sub>2</sub> nanoparticles made from biomaterials were used as antibacterial and antifungal agents. Using the well diffusion method, the antibacterial research of ZrO<sub>2</sub> NPs was conducted against various bacterial and fungi species. The results of the experiments demonstrated the effectiveness of the synthesis process and the appropriate use of ZrO<sub>2</sub> NPs as potent antibacterial and antifungal agents.

**Keywords:** *Caulerpa scalpelliformis* algae extract, Green synthesis, ZrO<sub>2</sub> NPs, X-ray diffraction, TEM, antibacterial applications.

## I. INTRODUCTION

One of the most active areas of modern materials science is the study of nanotechnology. Nanotechnology has emerged as a rapidly evolving field thanks to its uses in science and technology to create unique materials on a nanoscale. Typically, nanoparticles have they are a better candidate in terms of activity than their bulk counterparts because they have diameters between 1 and 100 nm and a higher surface area to volume ratio [1].

The so-called zirconium oxide, commonly known as zirconia, has drawn a lot of study interest due to its exceptional optical, electrical, mechanical, and biocompatible properties. It is a form of p-type semiconductor that exhibits both oxidizing and reducing abilities due to its acidic and basic composition [2]. Due to its exceptional qualities, it can be used for a variety of purposes, such as fuel cells, refractory materials, structural reinforcement, antibacterial agents, adsorption, and gas sensors.

As well as photo-degradation. Zirconia nanoparticles are created using physical and chemical processes such as hydrothermal, electrochemical, laser ablation, microwave irradiation, and photochemical [3]. However, the "biological or green synthesis" technique must quickly take their place due to the negative effects these procedures have on the environment [4]. As a result, the green synthesis method for creating nanoparticles appears promising. Compared to chemical and physical methods, green synthesis has a number of benefits, such as being less expensive, environmentally benign, and using less energy, heat, and harmful substances [5]. The biological method of synthesis uses microorganisms, fungi, algae, and plant extracts [6].

Plant extracts are very promising due to their intricate chemical makeup and extraction methods. The plant extract functions as a capping agent and a reducer in the synthesis, preventing the aggregation of nanoparticles during the stage of crystal development [7]. As a result, compared to microorganism-produced nanoparticles, those made from plant components are more stable and synthesize at a higher rate. Despite the fact that some scientists have used green synthesis to create zirconia nanoparticles [8], much more work is still required since plant species have such a wide genetic range that chemical composition might change significantly depending on the plant under study. This factor has a direct impact on the properties of the material obtained. As a result, it is still necessary to assess how different types are used [9]. The algae known as *Caulerpa scalpelliformis* algae is indigenous to the Tuticorin coast of Gulf Mannar, India. Its high phenolic content, and flavonoid content make it a highly effective reducing agent in the biological synthesis of ZrO<sub>2</sub> NPs [10].

Maximum significance is attached to the suggestion of a nanomaterial produced by green synthesis. Additionally, there is yet no information in the literature about the use of *Caulerpa scalpelliformis* algae extract as a reducer in the production of ZrO<sub>2</sub> NPs. In this study, zirconium nitrate (ZrO (NO<sub>3</sub>)<sub>2</sub>.H<sub>2</sub>O) was used to create ZrO<sub>2</sub> NPs using a green synthesis approach from *Caulerpa scalpelliformis* algae extract. High-resolution XRD was used to assess the prepared sample's crystalline quality, SEM was used to look at the surface shape, ENERGY-DISPERSIVE X-RAY SPECTROSCOPY (EDX) IS USED TO ANALYZE THE ELEMENTAL COMPOSITION OF SOLID SURFACES, AND TEM CAN BE USED TO STUDY THE GROWTH OF LAYERS, THEIR COMPOSITION AND DEFECTS IN SEMICONDUCTORS. Investigations are also made into UV-Vis absorption characteristics. Finally, zirconium dioxide nanoparticles' antibacterial activity was evaluated using the excellent diffusion method.

## 2. Experimental

### 2.1. Materials

The experiment employed only ultra-pure grade chemical reagents.

### 2.2. Preparation of *Caulerpa scalpelliformis* algae extract

The green algae *Caulerpa scalpelliformis* was collected from Tuticorin coast of Gulf Mannar, India. The collected biomass was washed thoroughly with tap water to clean up and shade-dried. The algal powder (1.0 g) was obtained by the grinder and extracted with distilled water at 60°C for 15 minutes. After cooling down of solution, until room temperature, the sample was centrifuged (1000 rpm) to remove debris. The obtained extract was stored at 4°C and used in the biosynthesis of ZrO<sub>2</sub>.

### 2.3. Preparation of ZrO<sub>2</sub> NPs using *Caulerpa scalpelliformis* algae extract

An aqueous solution of zirconium nitrate (0.5 M) was prepared by using dissolved 23.1 g of zirconium nitrate salt in 200 mL of DI water and heated at 80°C for 1 h with consistent stirring to get a white color solution. After that, 100 mL of pre-synthesized seaweed extract was added to the zirconium nitrate solution under a magnetic stirrer on a warm plate at 80°C for 1 h additionally. During the process, the shade of the extract response rapidly changed from pale yellow to darkish violet, indicating the formation of ZrO<sub>2</sub> NPs. After that, at room temperature, the finished solution became cooled. To produce a great powder from the prepared solution, 50 mL was put in a ceramic plate and the solution was evaporated at 250°C for three hours. The white powder produced was stored for further characterization in a sealed container.

### 2.4 Characterization

The crystalline segment and crystallite size of ZrO<sub>2</sub> NPs were determined via the usage of an X-ray Diffractometer instrument type (XRD, Shimadzu 6000, Japan) making use of CuK $\alpha$  radiation ( $\lambda = 1.5406 \text{ \AA}$ ) via use of test from 10° to 45°. To discover functional groups, a Fourier Transform Infrared Spectrophotometer (FTIR, Shimadzu 8000) was used. The morphology and particle size of synthesized ZrO<sub>2</sub> NPs sample were investigated by a TEM (JEOL JEM 2100). The elemental composition of synthesized ZrO<sub>2</sub> NPs was obtained by EDS attached to SEM (Carl-Zeiss), Model LEO 1430 VP, Germany. Optical absorbance for NPs was gained through (UV-Vis) spectrophotometer (kind Shimadzu, UV-1800) at room temperature.

## 3. Antimicrobial activity

The Agar diffusion approach was used to take a look at the antibacterial interest of the synthesized ZrO<sub>2</sub> NPs. This method was used against gram-positive bacteria and gram-negative bacteria *Aspergillus niger*, *Klebsiella pneumoniae*, *Escherichia coli*, *Bacillus subtilis*, and *Staphylococcus aureus* respectively. Different concentrations of ZrO<sub>2</sub> NPs (25, 50, and 100 µg/ml) were used in every dish. All the dishes were incubated for (24 h) at (37 °C) after which respective inhibition areas were measured. After 24 h, by way of measuring the diameter of the inhibition zone surrounding each well the effectiveness of every concentration was calculated.

### 3.1 Population and Sample

KSE-100 index is an index of 100 companies selected from 580 companies on the basis of sector leading and market capitalization. It represents almost 80% weight of the total market capitalization of KSE. It reflects different sector company's performance and productivity. It is the performance indicator or benchmark of all listed companies of KSE. So it can be regarded as universe of the study. Non-financial firms listed at KSE-100 Index (74 companies according to the page of KSE visited on 20.5.2015) are treated as universe of the study and the study has selected sample from these companies.

The study comprised of non-financial companies listed at KSE-100 Index and 30 actively traded companies are selected on the basis of market capitalization. And 2015 is taken as base year for KSE-100 index.

### 3.2 Data and Sources of Data

For this study secondary data has been collected. From the website of KSE the monthly stock prices for the sample firms are obtained from Jan 2010 to Dec 2014. And from the website of SBP the data for the macroeconomic variables are collected for the period of five years. The time series monthly data is collected on stock prices for sample firms and relative macroeconomic variables for the period of 5 years. The data collection period is ranging from January 2010 to Dec 2014. Monthly prices of KSE -100 Index is taken from yahoo finance.

### 3.3 Theoretical framework

Variables of the study contains dependent and independent variable. The study used pre-specified method for the selection of variables. The study used the Stock returns as dependent variable. From the share price of the firm the Stock returns are calculated. Rate of a stock salable at stock market is known as stock price.

### 3.1. Results and discussion

#### 3.2. X- Ray Diffraction (XRD) analysis

X-ray diffraction (XRD) sample of the green synthesized ZrO<sub>2</sub> NPs is proven in Fig. 1. The statistics well-known shows two forms of crystalline section viz. Monoclinic and tetragonal for ZrO<sub>2</sub> NPs. The distinguishing feature peaks for tetragonal-ZrO<sub>2</sub> occur at  $2\theta = 30.61, 34.83, 50.41$  and  $60.33$  corresponding to the (101), (110), (200) and (211) reflections having space institution  $P4_2/nmc$  and cell dimensions  $a = 3.591$  and  $c = 5.182 \text{ \AA}$  [JCPDS No. 79-1769]. Further peaks arise at  $2\theta = 31.56, 45.54, 63.14, 74.67$  corresponding to the (111), (211), (113) and (222) indicating the formation of the monoclinic crystal segment of ZrO<sub>2</sub> having area organization  $P2_1/a$  [11] and cell dimensions  $a = 5.309, b = 5.207$  and  $c = 5.1424 \text{ \AA}$  [JCPDS No. 37-1484]. It may be seen from the figure that the (101) plane has the highest depth revealing the orderly boom crystallites along the (101) plane. The common crystallite size "D" has been predicted to be 5.9 nm the use of the Scherer formulation (Eq. (1))

$$D = 0.9 \lambda / \cos \theta \quad (1)$$

where  $\lambda = 1.5406 \text{ \AA}$  (wavelength of the target Cu-K $\alpha$ ),  $\theta$  is the Bragg's diffraction angle, and  $\beta$  is the full width at half maximum (FWHM) of the diffraction peak [12-14].

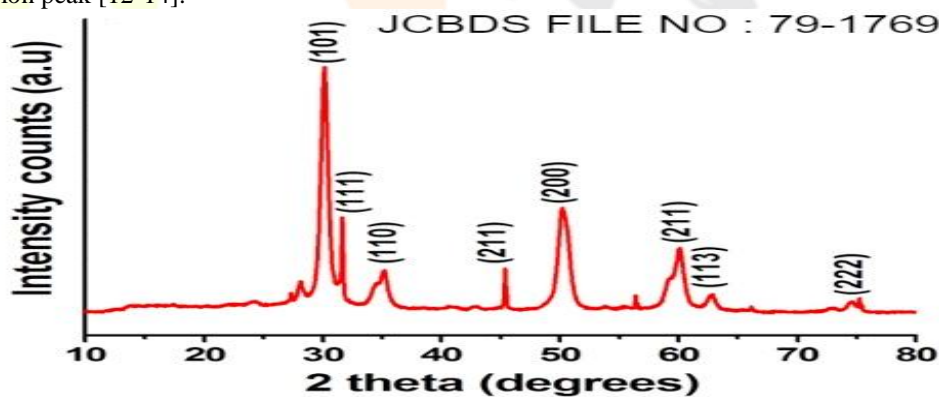


Fig. 1 XRD pattern of ZrO<sub>2</sub> NPs

#### 3.3. Fourier Transform Infrared (FTIR) analysis

FTIR spectrum of the ZrO<sub>2</sub> NPs is shown in Fig. 2. The observed broad band at the regions of  $3468 \text{ cm}^{-1}$  is due to asymmetric stretching of the OH group of the adsorbed moisture and interacting hydrogen bonds. The consistent peaks at  $1572$  and  $1355 \text{ cm}^{-1}$  are due to bending vibrations of -(H-O-H)- and -(O-H-O)- bonds. The prominent peak at  $1056 \text{ cm}^{-1}$  corresponds to C-O stretching vibrations. The characteristic bands at  $854$  and  $514 \text{ cm}^{-1}$  indicate the presence of Zr-O-Zr bending vibration which confirms the formation of ZrO<sub>2</sub> structure [12 and 15].

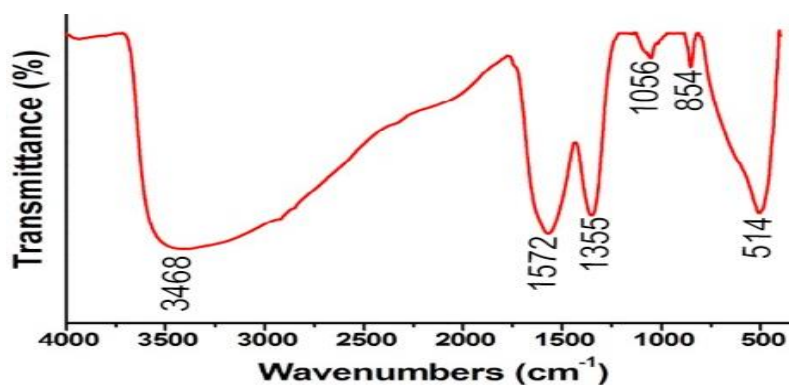


Fig. 2 FT-IR Spectrum of ZrO<sub>2</sub> NPs

#### 3.4 UV-visible absorption spectrum

Optical absorption measurement was also accomplished on ZrO<sub>2</sub> nanoparticles. Figure 3a shows the deviation of the optical absorbance with the wavelength of the ZrO<sub>2</sub> nanoparticles as prepared. The optical absorption coefficient was computed in terms of wavelength range of 300– 700 nm. It can be observed that the absorption edge is slightly red-shifted as distinguished from bulk ZrO<sub>2</sub>, thus approaching its absorption into the visible region. Hence, the samples are completely transparent at higher wavelengths. The UV spectrum exhibits an absorption peak at 254 nm which occurs due to a valence-to-conduction band transition.

$$(\alpha h\nu = A(h\nu - E_g)^{1/2}$$

The accurate band gap of ZrO<sub>2</sub> found to be 4.9 eV, which was obtained by plotting of  $(\alpha h\nu)^2$  versus photon energy ( $h\nu$ ) as shown in Fig. 3b. The observed band gap value is similar to the value reported in the literature [16].

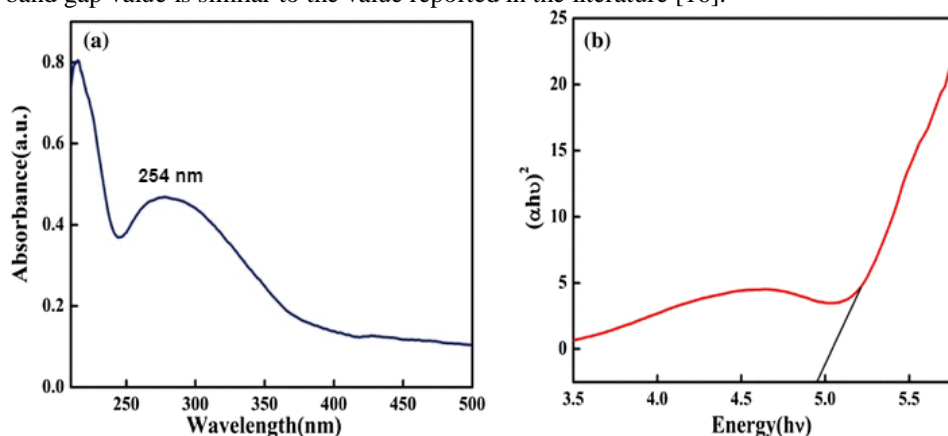


Fig. 3a Uv-Visible spectrum of ZrO<sub>2</sub> NPs and 3b Tauc plot of ZrO<sub>2</sub> NPs

### 3.3 Scanning electron microscopy (SEM) analysis

Figure 4 shows the SEM images of the as-prepared ZrO<sub>2</sub> nanoparticles. Due to aggregating or overlapping of smaller particles there are some larger particles. The SEM pictures clearly exhibit that the grains are randomly distributed with smaller size and it is noticed that the particles are of homogeneous spherical shape. The image clearly indicates that the average crystalline size could be 10 nm.

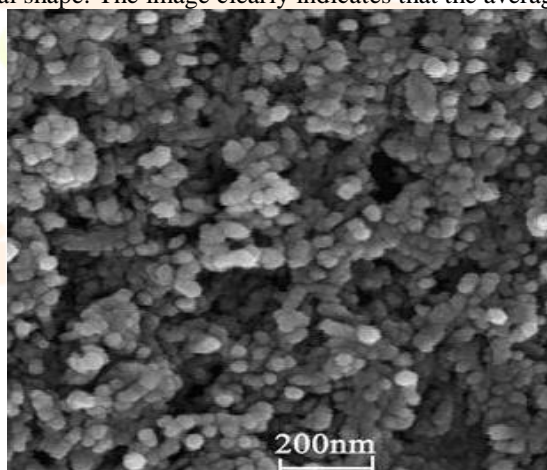


Fig. 4 SEM image of the ZrO<sub>2</sub> NPs

### 3.5 Energy dispersive X-Ray (EDX) composition analysis

Figure 5 shows an elemental examination of the ZrO<sub>2</sub> nanoparticles, in which the peaks of Zr and O are evident. The confirmation for the formation and composition of crystalline ZrO<sub>2</sub> nanoparticles was done by quantitative analysis, which showed the Zr and O as the only elementary species present in the sample signifying the high purity and the absence of any other impurity in the sample.

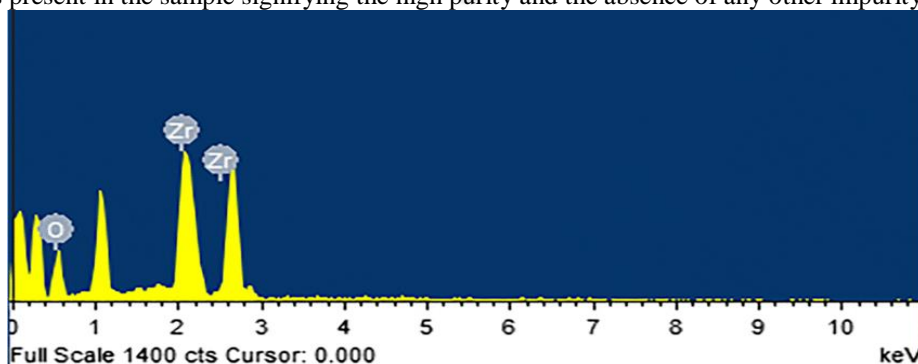


Fig. 5 EDX image of the ZrO<sub>2</sub> NPs

### 3.6 Transmission electron microscopy (TEM)

TEM is commonly used for imaging and analytical characterization of the nanoparticles to assess the shape, size, and morphology. TEM images of the ZrO<sub>2</sub> nanoparticles are shown in Fig. 6a. From the micrographs the average size of the particles was found to be a 15 nm and it was directly measured from the ruler of the image (Fig. 6b). Hence, the crystallographic studies obtained by TEM are in agreement with the corresponding XRD data.

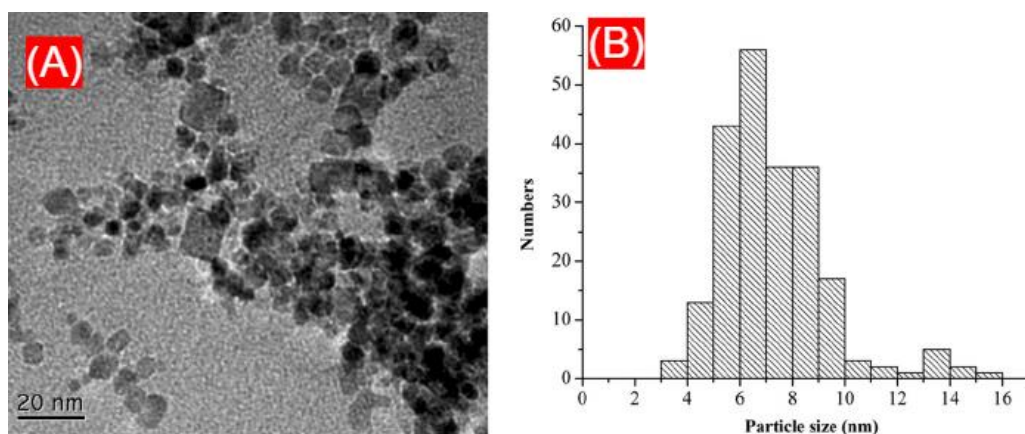


Fig. 6a TEM images of ZrO<sub>2</sub> nanoparticles and Fig. 6b Histogram of ZrO<sub>2</sub> NPs with size distribution

#### 4. Antimicrobial activity

In 2013, 9.2 million deaths were reported global. The motives at the back of the hundreds of thousands of deaths had been microbial infections [17]. Antibiotics participate in the remedy of infectious illnesses for the past 60 years. Over the past several many years, there may be additionally a boom inside the variety of dangerous species and antibiotic-resistant bacteria. Since the bacteria have many mechanisms for drug resistance, overcoming the situation has been tough for several industries [18]. To overcome antibiotic resistance, numerous researches have been conducted in recent years. Nanoparticles have appropriate inhibitory results against many kinds of bacterial traces and fungi. In this look at, the inhibitory activity of nanoparticles turned into evaluated with the aid of well diffusion approach in opposition to *Aspergillus niger*, *Klebsiella pneumoniae*, *Escherichia coli*, *Bacillus subtilis* and *Staphylococcus aureus* as shown in Table 1 and Fig. 7a. The effects proved that ZrO<sub>2</sub>NPs using *Caulerpa scalpelliformis* algae extract had an excellent inhibitory movement against Gram-positive quality bacteria [*B. Subtilis* (15 mm) and *S. Aureus* (14 mm)], Gram-negative bacteria [*K. Pneumonia* (17 mm) and *Escherichia coli* (15 mm)] and fungal stress [*A. Niger* (19 mm)], respectively (Fig. 7a). The nanoparticles confirmed the most zone of inhibition even on the minimal attention, which became in agreement with the earlier reports [19 and 20]. In Gram-negative bacteria, the anionic cell wall of bacteria would had been broken with the aid of the cationic zirconium ions and, hence, the produced ZrO<sub>2</sub>NPs using had shown higher antibacterial effects, which have been additionally mentioned earlier for silver nanoparticles [21]. The discount inside the intracellular ATP tiers could reason the impairment inside the outer and plasma membranes. The membrane proteins had deteriorated finishing up in cell harm and dying [22]. Thus, ZrO<sub>2</sub> NPs deem to be a capable antimicrobial agent in opposition to both bacteria and fungi.

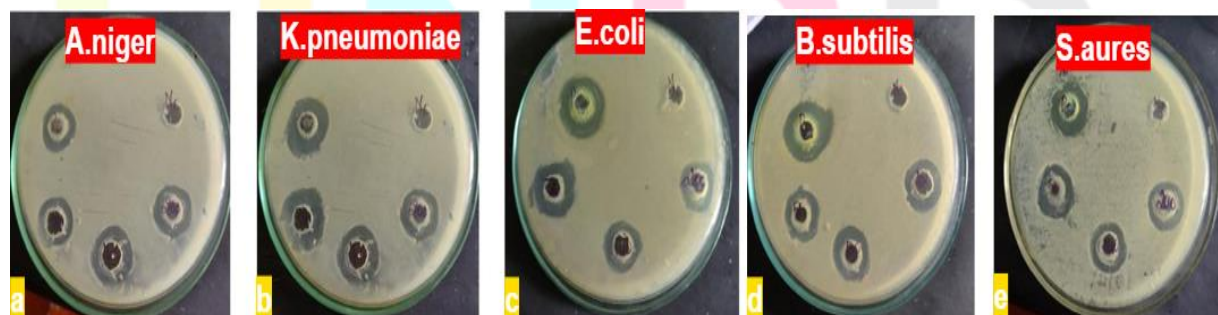


Fig. 7 a Zones of inhibition by the synthesized ZrO<sub>2</sub> nanoparticles against the test pathogens,

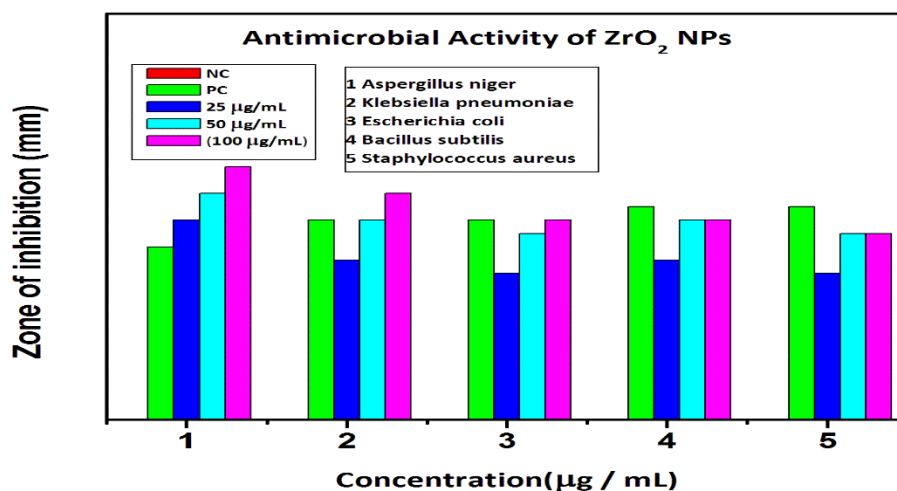


Fig.7b antimicrobial activity graph of the synthesized ZrO<sub>2</sub> nanoparticles

**Table 1 Antimicrobial activity of ZrO<sub>2</sub> nanoparticles**

Organism	PC	NC	25 (µg/mL)	50 (µg/mL)	100 (µg/mL)
Aspergillus niger	13	-	15	17	19
Klebsiella pneumoniae	15	-	12	15	17
Escherichia coli	15	-	11	14	15
Bacillus subtilis	16	-	12	15	15
Staphylococcus aureus	16	-	11	14	14

*PC positive control, NC negative control*

## 5. Conclusion In summary

*Caulerpa scalpelliformis* algae extract based ZrO<sub>2</sub> NPs have found excellent antimicrobial agents. The seaweed extracts were examined by means of different chemical test; examined secondary metabolites were responsible for bio-reduction, stabilization and capping of nanoparticles. The synthetic green method was low cost, eco-friendly and efficient. Biobased ZrO<sub>2</sub> NPs were analyzed by using UV-VISIBLE, FTIR, XRD, SEM, EDX and TEM method. Biosynthesis of ZrO<sub>2</sub> NPs were found highly effective to *Aspergillus niger*, *Klebsiella pneumoniae*, as compared to other bacterial and fungal strains. Therefore, the green synthesized ZrO<sub>2</sub> NPs can be used for antibacterial applications.

## REFERENCES

- [1] C. Noorjahan, S. Shahina, T. Deepika, S. Rafiq, Green synthesis and characterization of zinc oxide nanoparticles from Neem (*Azadirachta indica*), Int. J. of Sci. Eng. and Technol. Res. 4 (2015) 5751-5753.
- [2] A. Silva, A. Fagundes, D. Macuvele, E. Carvalho, M. Durazzo, N. Padoin, C. Soares, H. Riella, Green synthesis of zirconia nanoparticles based on *Euclea natalensis* plant extract: Optimization of reaction conditions and evaluation of adsorptive properties, Colloids and Surf. A: Physicochemical and Engineering Aspects. 583 (2019) 123915.
- [3] N. Pandiyan, M. Balaji, S. Jegatheeswaran, S. Selvam, M. Sundrarajan, Facile biological synthetic strategy to morphologically aligned CeO<sub>2</sub>/ZrO<sub>2</sub> core nanoparticles using *Justicia adhatoda* extract and ionic liquid: enhancement of its bio-medical properties, J. Photochem. Photobiol. B: Biology. 178 (2018) 481-488.
- [4] H. Salam, P. Rajiv, M. Kamaraj, P. Jagadeeswaran, S. Gunalan, R. Sivaraj, Plants: green route for nanoparticle synthesis, Int. Res. J. Biol. Sci. 1 (2012) 85-90.
- [5] P. Raveendran, J. Fu, S. Wallen, Completely "green" synthesis and stabilization of metal nanoparticles, J. of the American Chem. Society. 125 (2003) 13940-13941.
- [6] S. Vijayakumar, B. Vaseeharan, B. Malaikozhundan, M. Shobiya, *Laurus nobilis* leaf extract mediated green synthesis of ZnO nanoparticles: characterization and biomedical applications, Biomed. Pharmacother. 84 (2016) 1213-1222.
- [7] M. Abid, D. Kadhim, Novel comparison of iron oxide nanoparticle preparation by mixing iron chloride with henna leaf extract with and without applied pulsed laser ablation for methylene blue degradation, J. Environmen. Chem. Eng. 8 (2020) 104138.
- [8] A. Maroyi, Review of Ethnomedicinal Uses, Phytochemistry and Pharmacological Properties of *Euclea natalensis* A. DC, Mol. 22 (2017) 2128.
- [9] M. Shah, D. Fawcett, S. Sharma, S. Kumar Tripathy, G. Poinern, Green synthesis of metallic nanoparticles via biological entities, Mater. 8 (2015) 7278-7308.
- [10] D. Mahendiran, G. Subash, D. Selvan, D. Rehana, R. Kumar, A. Rahiman, Biosynthesis of zinc oxide nanoparticles using plant of *Aloe vera* and *Hibiscus sabdariffa*: Phytochemical, antibacterial, antioxidant and anti-proliferative studies, J. Bionanosci. 7 (2017) 530-545.
- [11] Y.W. Chen, J. Moussi, J.L. Drury, J.C. Wataha, Zirconia in biomedical applications, Expert Rev. Med. Devices (2016) 1-19.
- [12] S. Mallik, S.S. Dash, K.M. Parida, B.K. Mohapatra, Synthesis, characterization, and catalytic activity of phosphomolybdic acid supported on hydrous zirconia, J. Colloid Interface Sci. 300 (2006) 237-243.
- [13] S. Kumar, S. Kumar, S. Tiwari, S. Srivastava, M. Srivastava, B.K. Yadav, S. Kumar, T.T. Tran, A.K. Dewan, A. Mulchandani, J.G. Sharma, Biofunctionalized nanostructured zirconia for biomedical application: a smart approach for oral cancer detection, Adv. Sci. 2 (2015) 1-9.
- [14] C. Shuai, P. Feng, B. Yang, Y. Cao, A. Min, S. Peng, Effect of nano-zirconia on the mechanical and biological properties of calcium silicate scaffolds, Int. J. Appl. Ceram. Technol. 12 (2015) 1148-1156.
- [15] A.K. Singh, U.T. Nakate, Microwave synthesis, characterization, and photoluminescence properties of nanocrystalline zirconia, Sci. World J. 2014 (2014) 1-7.
- [16] L. Xie, J. Wang, Y. Hu, S. Zhu, Z. Zheng, S. Weng, P. Liu, RSC Adv. 2, 988 (2012).
- [17] Khameneh B, Iranshahy M, Soheili V, Bazzaz BSF (2019) Review on plant antimicrobials: a mechanistic viewpoint. Antimicrob Resist Infect Control 8:118.
- [18] Saleem M, Nazir M, Ali MS, Hussain H, Lee YS, Riaz N, Jabbar A (2010) Antimicrobial natural products: an update on future antibiotic drug candidates. Nat Prod Rep 27:238-254.
- [19] Kasithevar M, Periakaruppan P, Muthupandian S, Mohan M (2017) Antibacterial efficacy of silver nanoparticles against multi-drug resistant clinical isolates from post-surgical wound infections. Microb Pathog 107:327-334.
- [20] Suganya KU, Govindaraju K, Kumar VG, Dhas TS, Karthick V, Singaravelu G, Elanchezhian M (2015) Size controlled biogenic silver nanoparticles as antibacterial agent against isolates from HIV infected patients. Spectrochim Acta Part A Mol Biomol Spectrosc 144:266-272

[21] Emmanuel R, Palanisamy S, Chen S-M, Chelladurai K, Padmavathy S, Saravanan M, Prakash P, Ali MA, Al-Hemaid FM (2015) Antimicrobial efficacy of green synthesized drug blended silver nanoparticles against dental caries and periodontal disease-causing microorganisms. *Mater Sci Eng, C* 56:374–379.

[22] Arokiyaraj S, Vincent S, Saravanan M, Lee Y, Oh YK, Kim KH (2017) Green synthesis of silver nanoparticles using *Rheum palmatum* root extract and their antibacterial activity against *Staphylococcus aureus* and *Pseudomonas aeruginosa*.

